COURSE ON VEHICLE AERODYNAMICS

Prof. Tamás Lajos
University of Rome "La Sapienza" 1999

1. Introduction

Subject of the course: basics of vehicle aerodynamics ⇒ ground vehicle aerodynamics ⇒ examples in car, bus, truck aerodynamics.

Main objectives of vehicle aerodynamics:
- reduction of drag and fuel consumption,
- improvement of operational characteristics (stability, safety, handling characteristics)
- improvement of comfort characteristics (noise generation, mud deposition etc.)

3 flow fields: - flow past vehicle bodies,
- flow in passenger compartment (ventilating, heating),
- flow in and around components (cooler, brakes etc.)

2. History

4 periods:
- 1900 -1920 *Adaptation of the form* of different vehicles (e.g. boats and airships) and devices like bodies (e.g. torpedoes),
- 1920 -1970 Utilisation of the *results of aeroplane aerodynamics*. Gap between aerodynamic achievements and the mass production of cars. Pál Járay, Klemperer: optimum body shape near the ground, car bodies constructed by combining wing and airship sections. Kamm: cut of long tail of Járay's cars.
- 1970 - *Form optimisation*: starting from a given car body configuration meeting the needs of consumers, technological, styling and safety requirements etc. and changes of body shape will be carried out to improve the aerodynamic characteristics.
- 1980 - Development of aerodynamically *optimal body shape* and its use as the starting point for the development of a car body.

3. Forces and moments

The forces and moments acting on a car body:

where:
D drag
L lift
S side force
M_Y yawing moment
M_P pitching moment
M_R rolling moment.

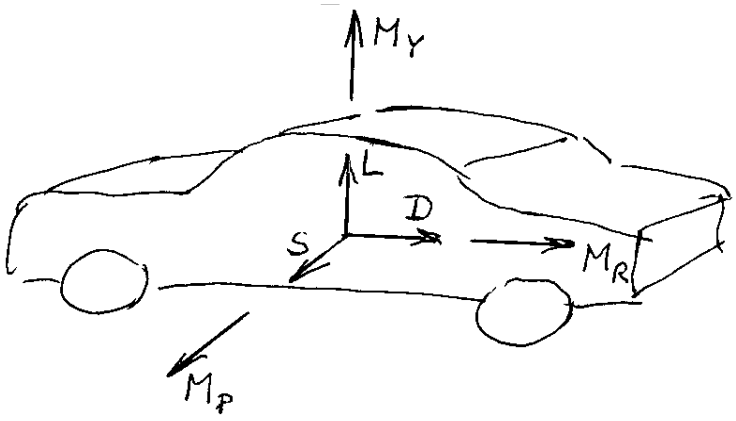

3.1. Regarding a given vehicle body shape, the following relation can be written between a force component (e.g. D) and the related physical quantities (undisturbed approaching velocity v, density ρ, dynamic viscosity μ, characteristic size (e.g. wheel base) L and angle of attack β: F (D, v_∞, ρ, μ, L β) = 0

Using Buckingham's Π theorem, 3 dimensionless groups can be formed:

$$\Pi_1 = \frac{D}{\frac{\rho}{2} v_{\infty\infty}^2 L^2} \qquad \Pi_2 = \frac{v_\infty L \rho}{\mu} = Re \qquad \Pi_3 = \beta$$

Since L^2 is proportional to the largest cross wind area A,

$$c_D = \frac{D}{\frac{\rho}{2} v_{\infty\infty}^2 A}$$

Where c_D is *drag coefficient* and Re is *Reynolds number*. Similar force coefficients can be defined: *lift-* and *side force coefficient*.

3.2. The *moment coefficients* are defined as follows:

$$c_Y = \frac{M_Y}{\frac{\rho}{2} v_\infty^2 A L}$$

yaw coefficient.

3.3. The possibilities of drag reduction

Cars:	c_D
- without any deeper aerodynamic considerations	0.5
- on the basis of literature	0.45
- with form optimisation and model experiments	0.4
- starting from an optimum body shape, long development	0.3
- future perspectives	0.2

Busses, trucks:
from c_D = 0.6 - 1 through aerodynamic developments c_D = 0.35 - 0.4.

4. Wind characteristics

Wind is generated by a pressure difference on the surface of the Earth. Because of the Coriolis forces caused by the rotation of the Earth and the relative velocity of the air, the streamlines of wind coincide approximately with the isobars. The thickness of the atmospheric boundary layer (gradient height) is z [m] where gradient velocity v_G prevails. The wind profile can be approximated by expression:

$$\frac{v}{v_G} = \left(\frac{z}{z_G} \right)^{1/n}$$

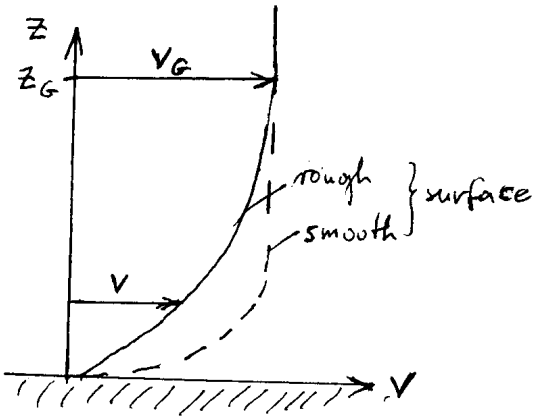

The turbulence of wind can be characterised by the gust factor:

$$F_{10}^{t} = \frac{\overline{v_{10}^{t}}}{\overline{v_{10}}}$$

where subscript 10 means the height of observation in [m] and t is the time of observation in [s]. So the gust factor is the quotient from the mean velocity for a time span t [s] and the mean velocity for one hour.

The main characteristics of atmospheric wind depend on the roughness of the Earth surface:

	smooth surface (e.g. lake)	rough surface (e.g. downtown)
z gradient height in m	200	550
1/n exponent	0.12	0.3
F^{3}_{10} gust factor	1.4	2

The roughness of the surface considerably increases the turbulence intensity. The wind influences the flow past vehicle bodies.

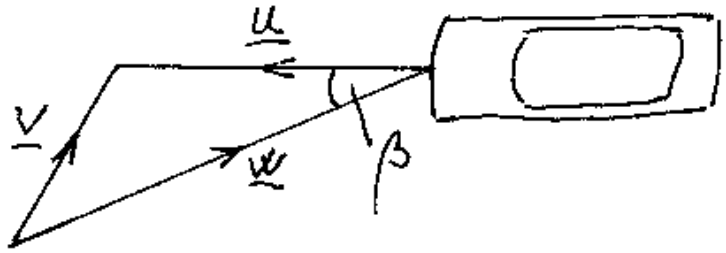

u vehicle velocity

v absolute (wind) velocity

w relative velocity

The consequences of the wind:
- the average drag and so the fuel consumption increases,
- the flow past vehicle body changes: angle of attack β differs from 0, twisted and in vertical direction changing approaching relative velocity profile,
- increased turbulence intensity depending on Tu of the wind and the v/w ratio,
- increased noise intensity.

5. Origin of forces and moments acting on bluff bodies

Bluff bodies are characterised by a separated flow covering large parts of their surfaces.

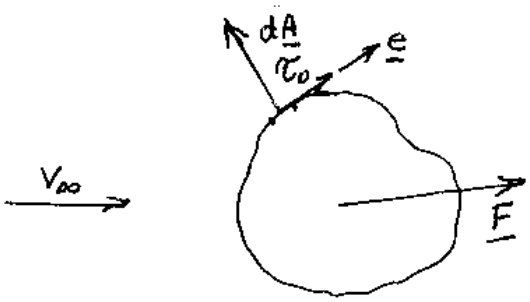

The force acting on a bluff body immersed in a parallel flow can be expressed:

$$\underline{F} = -\int_A p\,d\underline{A} + \int_A \tau_0\,\underline{e}\,|d\underline{A}|$$

where τ_0 [Pa] is the wall shear stress, $\underline{e}$ is a unit vector showing the direction of the local wall shear stress.

The forces and moments can be attributed to the pressure distribution and to the wall shear stress distribution.
The pressures and shear stresses can be characterised by the pressure and local friction coefficients: c_p and c'_f:

$$c_p = \frac{p - p_\infty}{\frac{\rho}{2} v_\infty^2} \qquad c_D = \frac{\tau_0}{\frac{\rho}{2} v_\infty^2}$$

The magnitudes of these coefficients differ very much. Usually:
$-2.5 < c_p \le 1$ and $|c'_f| < 0.01$.

Conclusion: the forces acting on bluff bodies are mainly caused by the pressure distribution. The immediate effects of wall shear stresses are quite small: the drag of streamlined bodies, where the shear stresses dominate (e.g. wings), is smaller by two order of magnitude than that of bluff bodies. **At bluff bodies the viscosity of the fluid exerts its influence not mainly through the forces caused by wall shear stresses but by influencing the flow field past bodies (e.g. by boundary layer separation) resulting unbalanced pressure distributions.**

6. Example: flow past cylinder

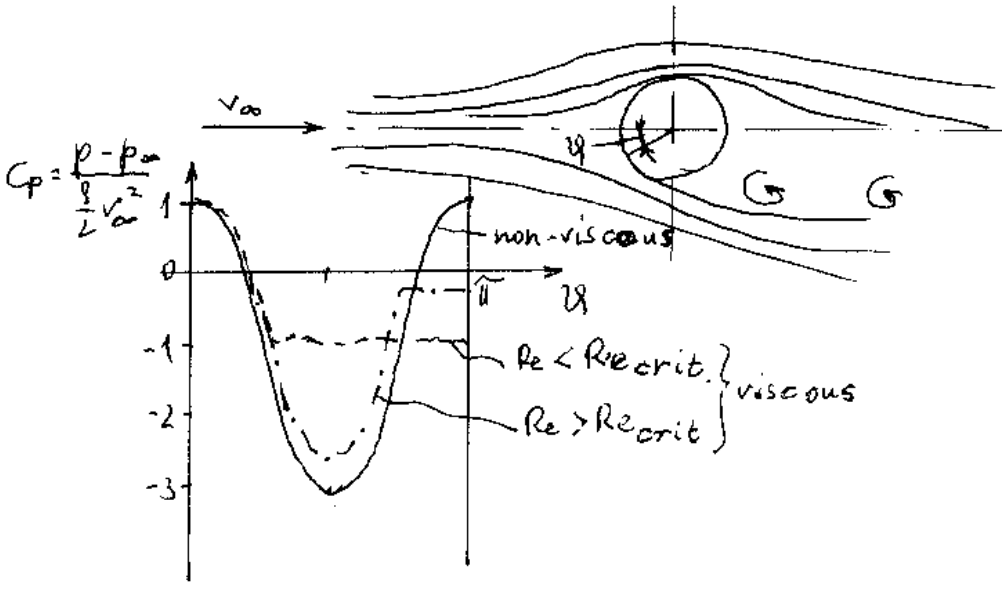

non-viscous

viscous

The real flow field shows asymmetry caused mainly by boundary layer separation. The pressure distribution on the front face is very close to that of non-viscous case.

Navier-Stokes equation:

$$\frac{d\underline{v}}{dt} = \underline{g} - \frac{1}{\rho}\,\mathrm{grad}\,p + \nu\,\Delta\underline{v}, \quad \text{where} \quad \Delta\underline{v} = \mathrm{grad}\,\mathrm{div}\,\underline{v} - \mathrm{rot}\,\mathrm{rot}\,\underline{v}.$$

In case of Incompressible fluid (div $\underline{v}$ = 0) the friction term of N.S. equation becomes: - ν rot rot $\underline{v}$. The viscosity of fluid plays no role in case of rot v = 0. Because of no-slip condition on solid walls near the wall, in boundary layer rot$\underline{v} \neq$ 0. The boundary layer remains thin in accelerating flow: over a part of the front of the cylinder the flow field is very similar to the flow developing in a non-viscous fluid.

Boundary layer separation causes substantial changes in the flow pattern past bluff bodies.

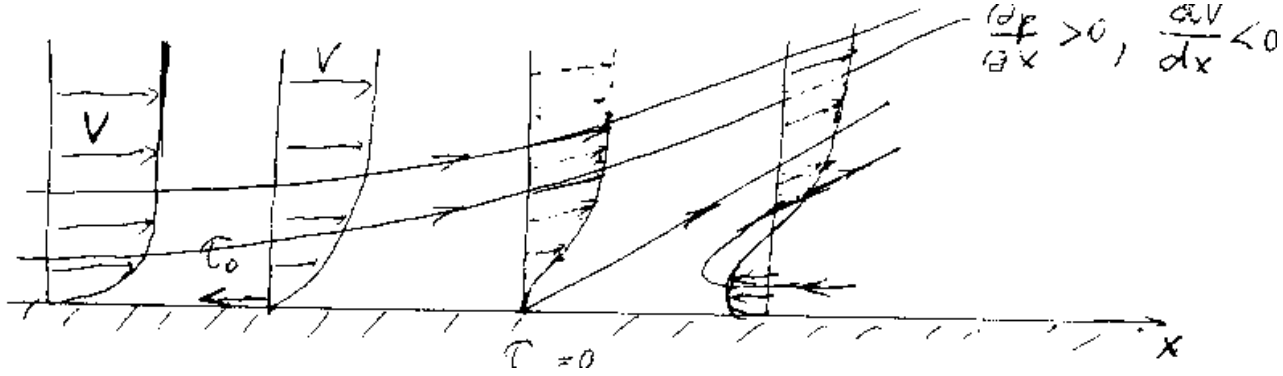

The two conditions for boundary layer separation are:
- vicinity of the wall,
- pressure increase downstream (adverse pressure gradient).

Boundary layer separates if the decelerating forces relating to the shear stresses on and near the wall and to the adverse pressure gradient exceed the impulse transport from outside flow into the boundary layer.

So the boundary layer separation can be stopped or influenced by
- reducing the shear stresses or making them disappear (e.g. by moving the wall τ_0 =0)
- decrease of adverse pressure gradient (e.g. by rounding up of edges)
- removal from boundary layer of slow fluid layer decelerated by adverse pressure gradient and by friction (e.g by boundary layer suction);
- increase of the impulse transport in the lower part of the boundary layer by
  - blowing in wall jet
  - laminar-turbulent transition (increase of Re number or increase of roughness)
  - increase of turbulent mixing by using turbulence generator.

The *pressure distribution* on a body can easily be assessed by using Euler equation in natural co-ordinate system. At steady, non-viscous flow and neglecting the forces acting on the mass of fluid (e.g. the weight), we obtain:

$$\frac{v^2}{r} = \frac{1}{\rho}\frac{\partial p}{\partial n},$$

where r[m] radius of curvature of the streamline, n co-ordinate perpendicular to the streamline.
That is:
- in case of straight streamlines (r = ∞) the pressure does not change perpendicular to the streamlines;
- for curved streamlines, the pressure increases perpendicularly to the streamlines when moving away from the centre of curvature.

The relation between *Reynolds number* and drag coefficient of the circular cylinder:

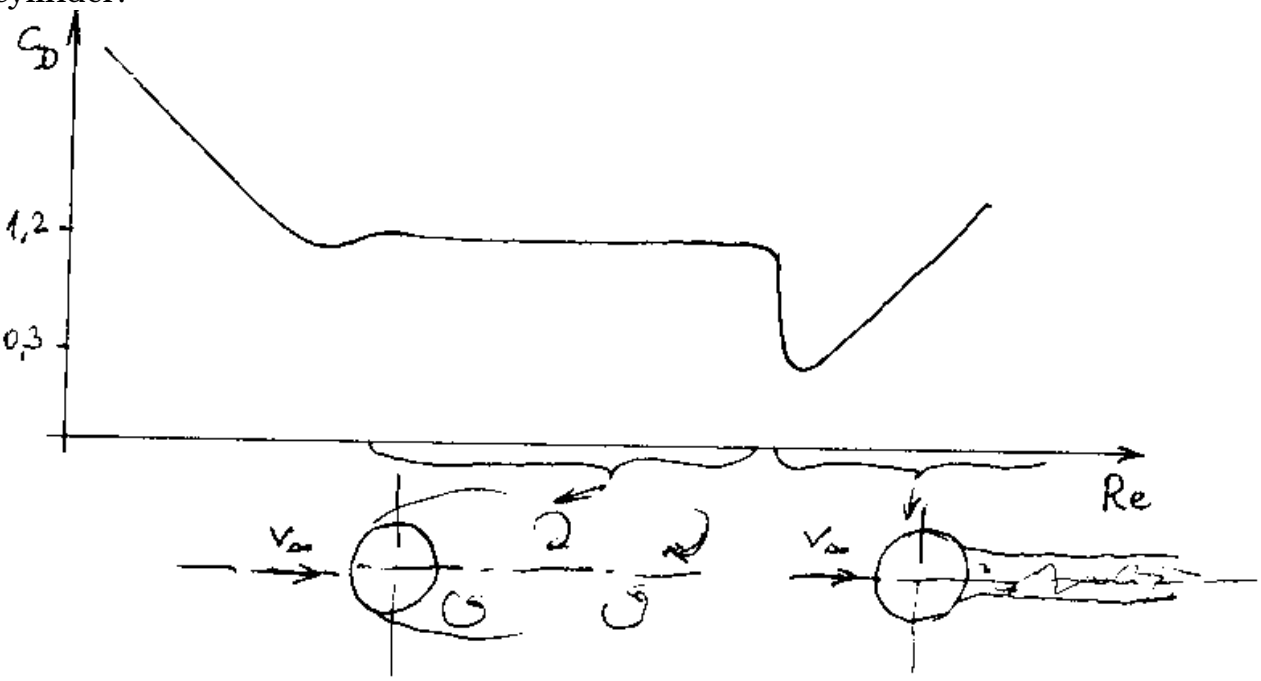

At small Reynolds numbers, the viscous forces dominate: $D \propto v_\infty \Rightarrow c_D \propto 1/ v_\infty \propto 1/Re$. At higher Reynolds number $D \propto v_\infty^2$ therefore c_D = const. At Re_{crit} dramatic decrease of c_D can be observed which is the consequence of laminar-turbulent transition in the boundary layer. (The line of boundary layer separation shifts downstream, therefore the wake will be much smaller, and the asymmetry of the pressure distribution decreases. Near Re_{crit} an increase of roughness of the surface of the cylinder can result in a laminar-turbulent boundary layer transition.

In the region c_D = const., regular vortex shedding occurs as a consequence of instability and rolling up of shear layer originating from the separation line as well as the interaction of shear layers developing on opposite sides of the cylinder.

The *aerodynamic forces* acting on bodies can be evaluated in two ways:

1. By observing the pressure and wall shear stress distribution on the surface of the body. (In this case, the presence of strong vortices in the vicinity of the rear part of the cylinder results in low base pressure and high drag.)
2. By observing the downstream flow field (the wake): the flow direction, velocity and total head distribution, and kinetic energy content of flow field. (In case of a cylinder at a given Reynolds number interval from the presence of large, strong and alternating downstream vortices, large drag and alternating lift can be concluded.)

The Karman vortex street can be stopped by using a splitter plate in the wake stopping the interaction of opposite shear layers:

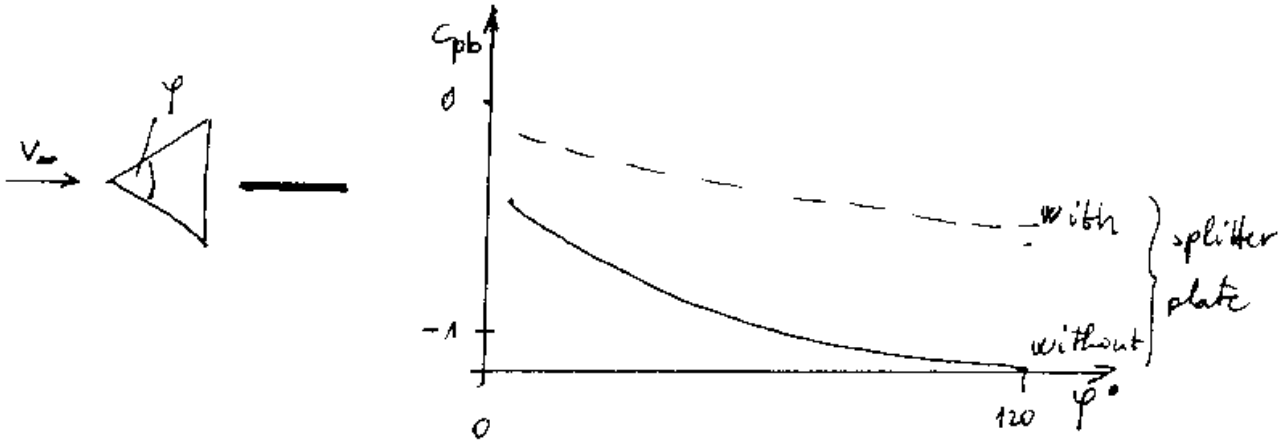

By stopping the rise of strong vortices, the base pressure coefficient c_{pb} increases (e.g. the drag decreases) considerably. Another conclusion can be drawn from the above diagram: the base pressure decreases with increasing angle of wedge, i .e. with increasing angle between the undisturbed flow and the tangent of the shear layer at the boundary layer separation (in this case this angle is ≈ φ/2).

7. 2D and 3D bodies

A flat plate of length l and width d is immersed in parallel flow perpendicular to the undisturbed flow. The drag coefficient, and mean pressure coefficients related to the front and the base of the plate for different l/d aspect ratios are as follows:

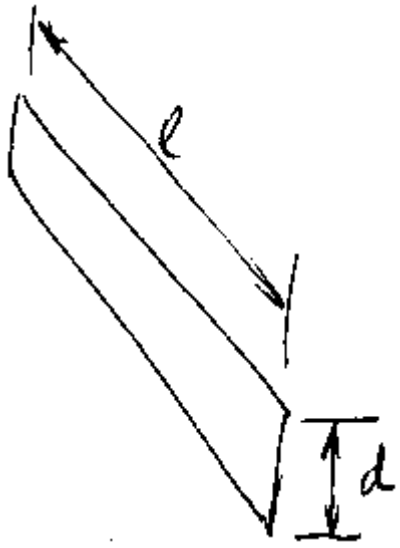

l/d	c_D	c_{pf}	c_{pb}
∞	2	0.8	-1.2
18	1.4		
4	1.19		
1	1.1	0.79	-0.31
		small	substantial change

The significant change of c_D is caused by decrease of base pressure. For aspect ratios l/d < 20 three dimensional character of flow increases. The flow around sides induced by pressure differences weakens the periodic shedding of strong vortices (similar effect as caused by a splitter plate).

In 3D flow field *no regular shedding of strong vortices* can be observed.

Flow past a brick shaped 3D bluff body.

$$D = (\overline{p_f - p_\infty})h^2 + 4hl\tau_0 - (\overline{p_b - p_\infty})h^2 \quad \Rightarrow c_D = \frac{D}{\frac{\rho}{2}v_\infty^2 h^2} = \overline{c_{pf}} + 4\frac{l}{h}c_f' - c_{pb}$$

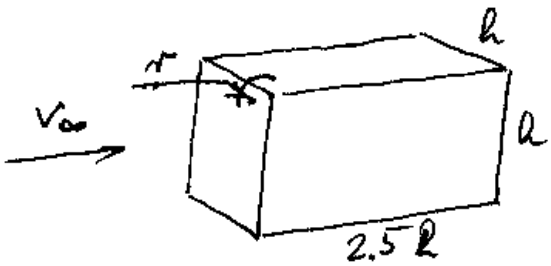

Carr's measurements on a brick shape body:

leading edges	sharp	rounded
r/h	0	0.3
c_D	0.88	0.2
$c_{pf,mean}$	0.57	- 0.03
$10c'_{f,mean}$	0.001	0.003
$c_{pb,mean}$	- 0.3	- 0.2

In absence of strong shedding vortices, the forebody drag ($c_{Df} = c_{pf,mean}$) plays an important role in c_D. Therefore in case of 3D bodies, the first task of the drag reduction is the reduction of the forebody drag.

8. ***Reduction of forebody drag***

The forebody drag is the consequence of an overpressure on the front face, so the forebody drag can be reduced by decrease of pressure on as large part of the front face as possible. The pressure can be reduced by accelerating the flow above the front face e.g. by rounding the leading edges surrounding the front face or by increasing the flow velocity around rounded leading edges by reducing the underbody flow. .

The pressure distribution on the front face of a quadratic brick shaped bluff body with sharp and rounded leading edges shows that the rounding of leading edges accelerates the flow and results in large suction on the periphery of the front face.

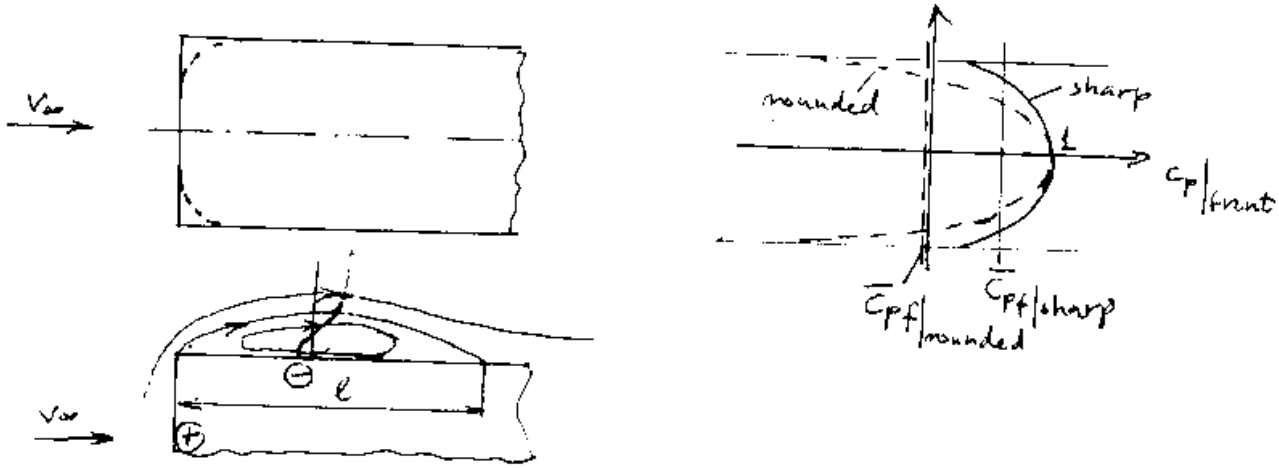

If the leading edge is sharp or the rounding radius is small, the adverse pressure gradient is too high. Therefore, the boundary layer separates and a separation bubble develops beside the side walls. *The length of the separation bubble l is a good indicator of the forebody drag.* (A linear relation has been found between c_D and l/h.) The flow turnaround the leading edge results in any case in a low pressure region. The forebody drag can be reduced by shifting this low pressure region at least partly over the front face.

Decreasing the adverse pressure gradient i.e. increasing the rounding can stop the boundary layer separation on the periphery edge. For full scale vehicles, r/h=0.05-0.1 proved to be sufficient (h characteristic cross-wind size of vehicle). At $Re_h = 3 \cdot 10^5$, the relation between r/h and c_D and the base drag ($c_{Db} = - c_{pb}$) is plotted in the following diagram:

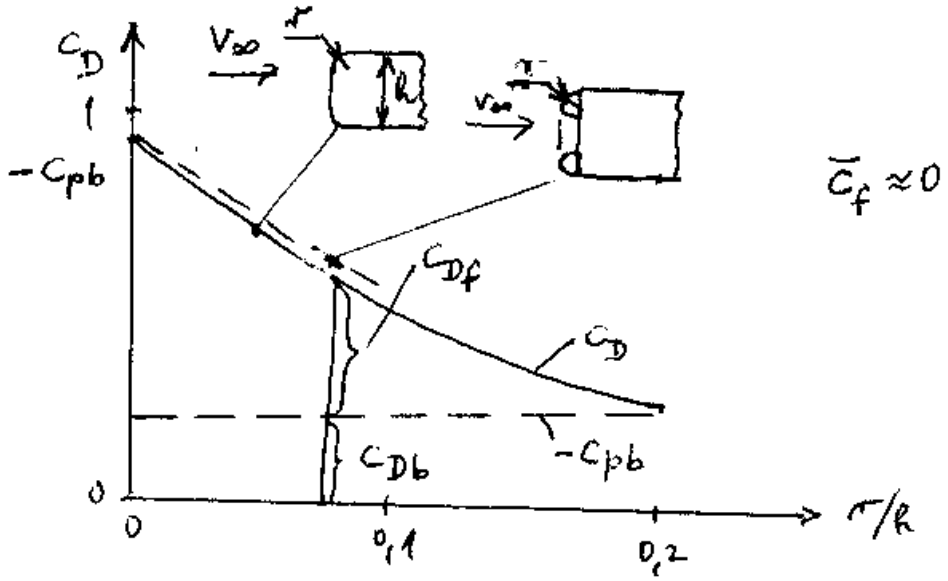

In case of rounded leading edges the drag is dominated by the base drag. The drag of the brick shape bluff body can be reduced by "add-on-devices", e.g. by a "lip" characterized by the rounding radius r.

An other add-on-device is the turning vane around the leading edge:

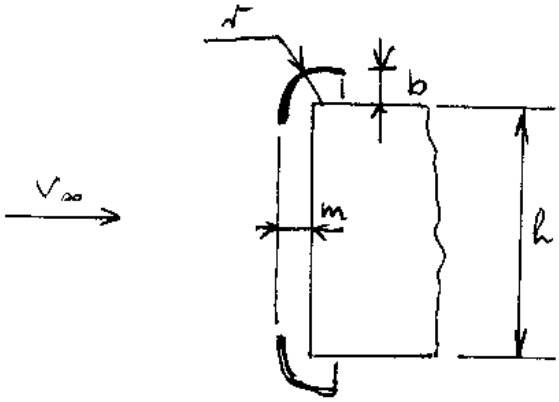

r/h=0.125, m/h=0.1, b/h=0.05. c_D =0.8 without turning vane, c_D =0.35 with turning vane. If the turning wane is disconnected from the body and it is held from outside c_D = 0.81. That means that the drag of bluff body is reduced by the forces acting on the vane, directed against the approaching flow.

The forebody flow can also be reduced by artificially creating a boundary layer separation on the periphery of the front face by using a "step" or a "fence". Near the separation bubble, a low pressure area is created decreasing the net force acting on the front face.

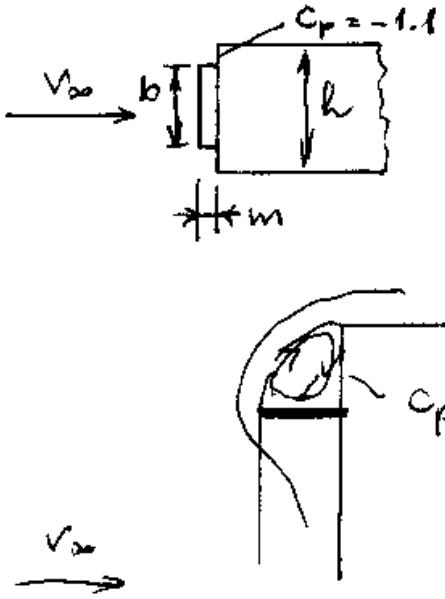

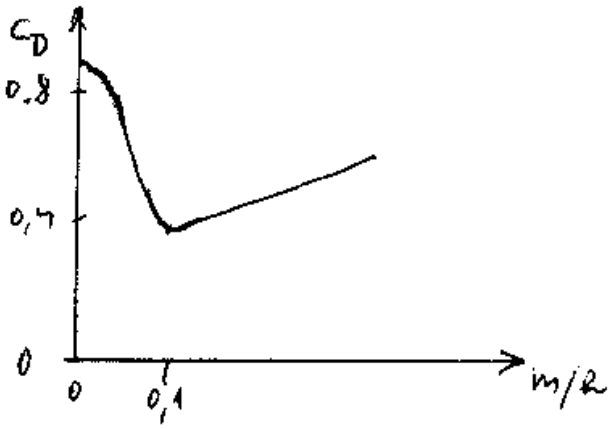

Practical application: "windshield spoiler" for buses: Δc_D =0.2, reduction of fuel consumption is 5-8%.

9. Characteristics of separation bubbles

Development of separation bubbles:
boundary layer separation ⇒ formation of shear layer ⇒ big velocity gradient across the shear layer ⇒ intense turbulent mixing ⇒ entrainment (fast moving fluid particles bring the slower particles with them) ⇒ supply of entrainment needs reverse flow ⇒ reverse flow needs pressure below the ambient ⇒ curvature of streamlines ⇒ re-attachment (or closing the bubble by contact of shear layers) ⇒ flow rate balance, feedback.

Main characteristics of separation bubble:
- there is a reverse flow (flow direction is opposite to the undisturbed approaching flow),
- the separation bubble is surrounded by solid surfaces and shear layers,
- the velocities are relatively small max 20-30% of undisturbed velocity,
- the pressure in the separation bubble is approximately constant and nearly equals the pressure at the separation point (line),
- no excessive periodic vortex shedding occurs,
- high turbulence intensity but definite flow structures which can be identified and reconstructed,
- the value of the pressure coefficient in the separation bubble depends on the angle φ between the undisturbed flow v_∞ and the tangent of the shear layer at the separation point.

φ decreases ⇒ c_{pb} increases ⇒ base drag c_{Db} decreases

10. The base drag

The rear parts of bodies are characterised by decelerated flow ⇒ boundary layer separation ⇒ development of extensive separation bubbles. The base drag (c_{Db}=-c_{pb}) can be reduced by increasing the pressure on the rear part of the body (most frequently the pressure in the separation bubble near the rear wall).

Brick shape bluff bodies of different lengths with quadratic cross section and sharp leading and trailing edges:

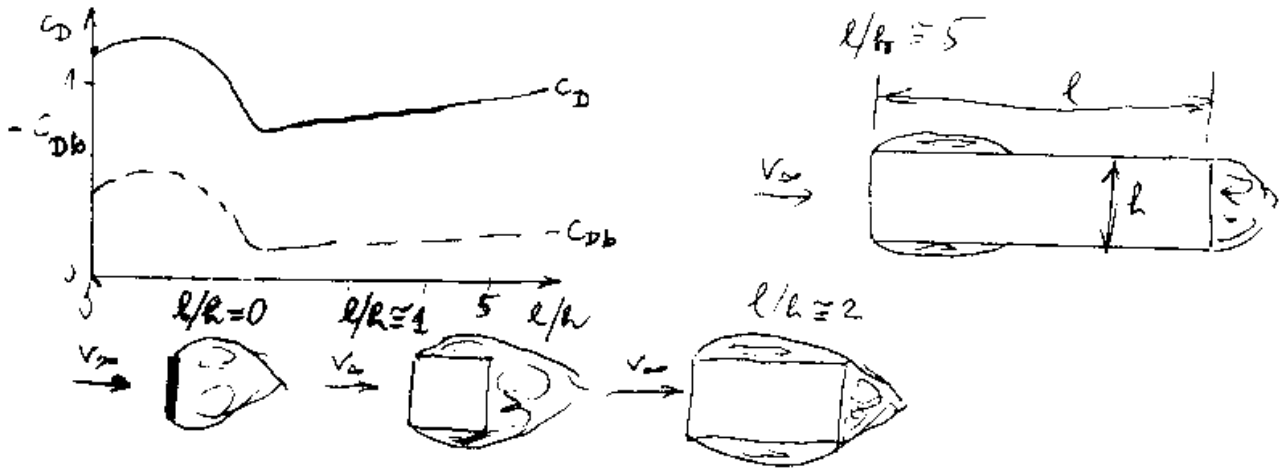

The drag is high, if the base of the body is in the separation bubble attached to the separation near the leading edge. (φ is large). If the base is in the separation bubble attached to the trailing edges, the base drag and so the overall drag is much smaller. Boat tailing: deceleration of flow (decrease of φ).

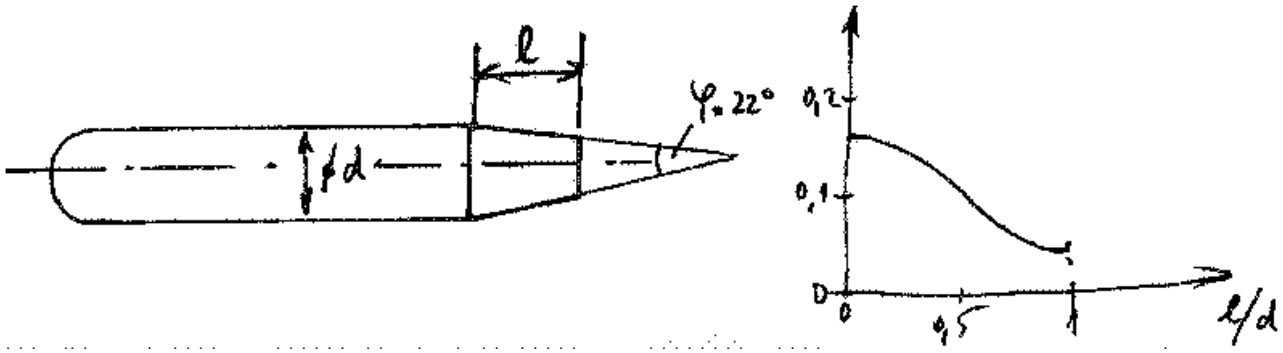

Rounding of trailing edge r/h=0 ⇒ 0.3 results in drag reduction:

if leading edge is sharp	r/h = 0	Δc_D = - 0.025
if the leading edge is rounded	r/h = 0.3	Δc_D = - 0.089

For rounded leading edge the flow past side walls of the bluff body is "sound" (no separation bubble besides them) that is why the rounding of the trailing edges is more efficient.

Slanting the rear wall can cause strong longitudinal vortices that reduce the pressure on the slanted surface. This results in an increase of drag and lift.

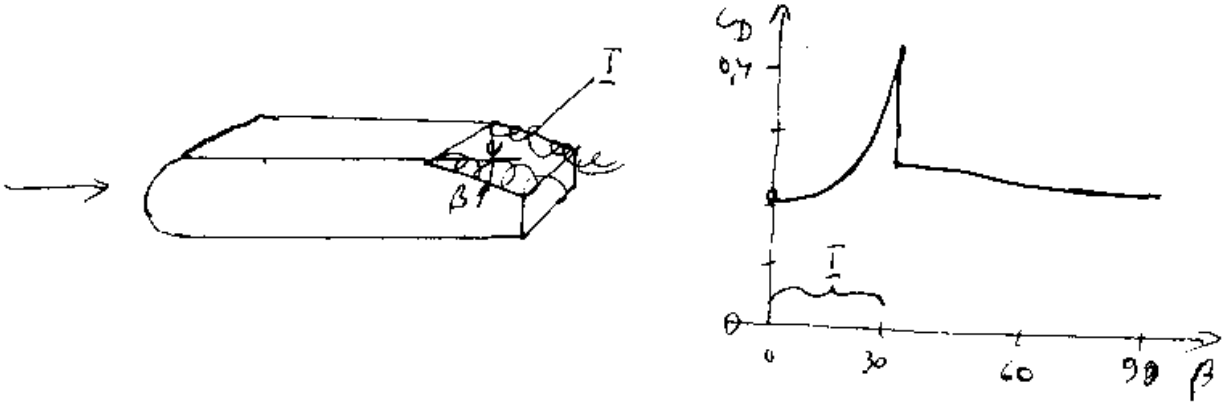

The side wind increases the separation bubble on the leeward side wall. If this separation bubble reaches the separation bubble behind the rear wall, the pressure in the merged separation bubbles will be lower than the initial pressure in the rear separation bubble, i.e. the drag decreases.

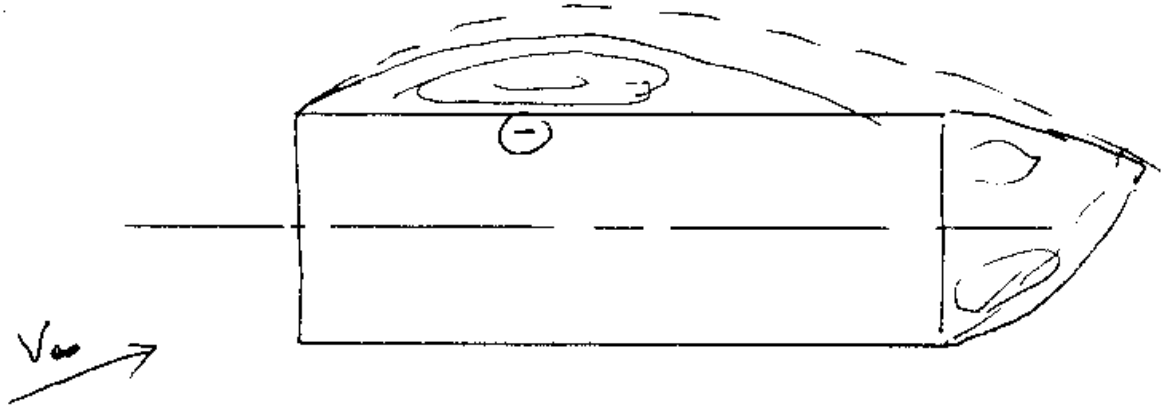

11. The ground effect

If the body approaches the ground the flow past body comes under the influence of its image. The vicinity of the ground stops the symmetry, lift and pitching moments are developed.

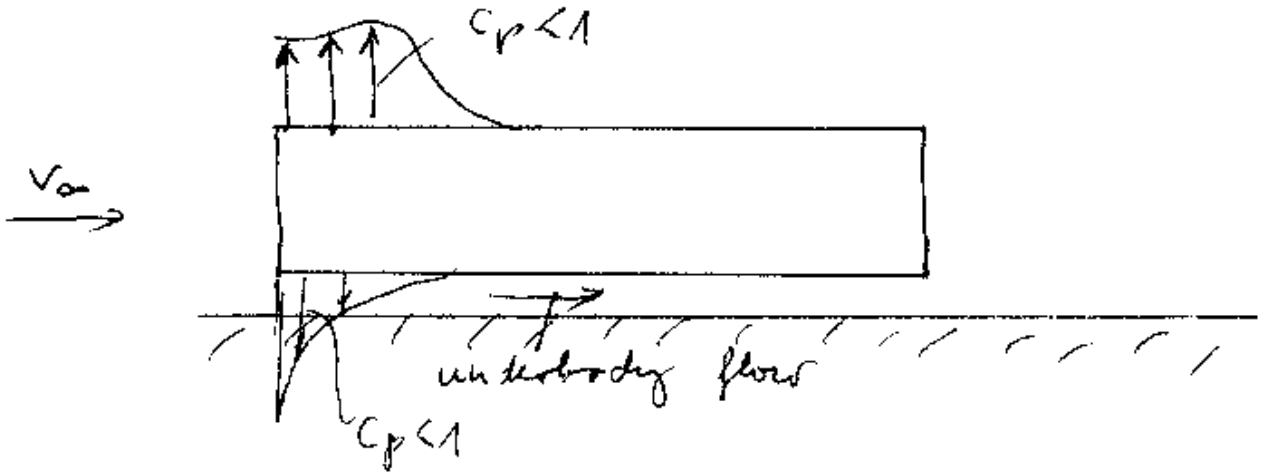

The underbody flow affects the rest of the flow past the bluff body:

- the underbody flow is decelerated by the (usually rough) underbody, therefore a part of it leaves the underbody gap on the sides,
- the angle outflow can cause strong longitudinal vortices and displace the sound flow beside the side walls,
- the rear outflow from the underbody gap can considerably influence the near wake.

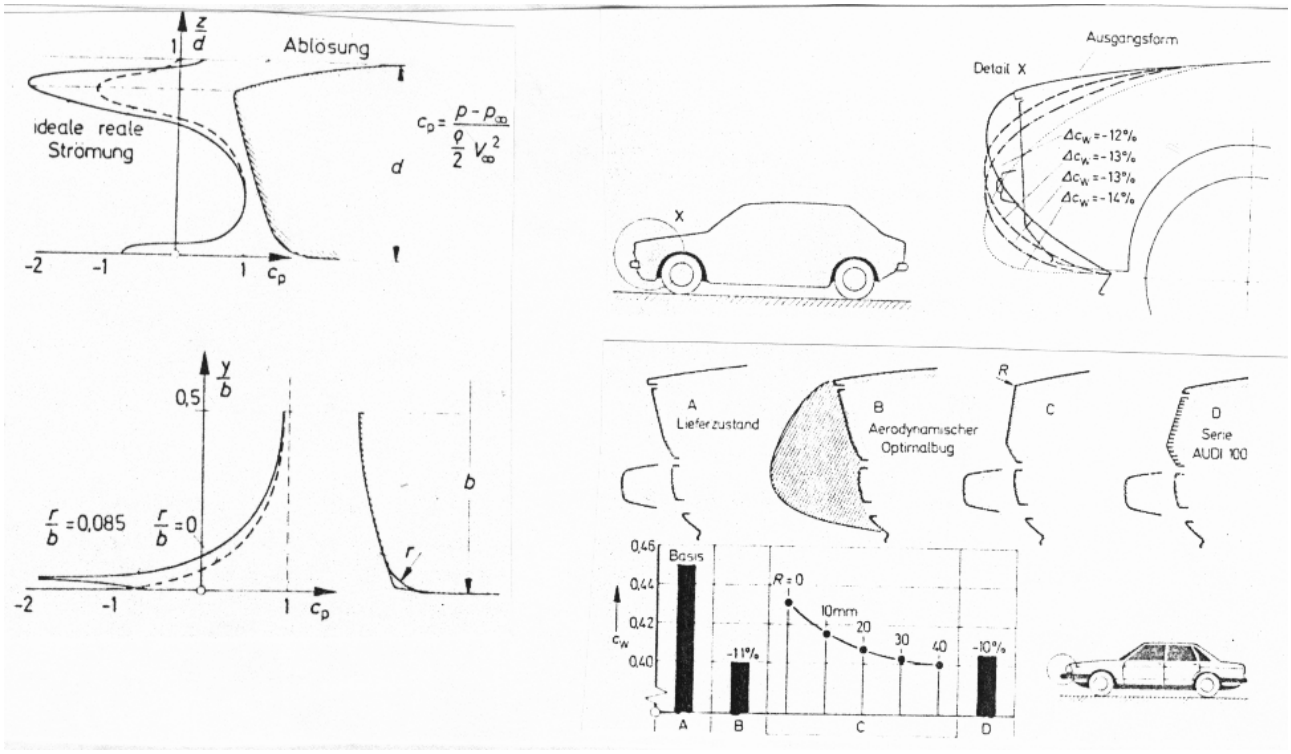
z/d
1
Ablösung
ideale reale Strömung
$c_p = \frac{p - p_\infty}{\frac{\rho}{2} V_\infty^2}$
d
-2
-1
1
c_p
y/b
0,5
r/b = 0,085
r/b = 0
b
r
Ausgangsform
Detail X
X
$\Delta c_W = -12\%$
$\Delta c_W = -13\%$
$\Delta c_W = -13\%$
$\Delta c_W = -14\%$
A
Lieferzustand
B
Aerodynamischer Optimalbug
C
R
D
Serie AUDI 100
0,46
0,44
0,42
0,40
c_W
Basis
-11%
R = 0
10mm
20
30
40
-10%
A
B
C
D